REMOVEDEBRIS – MISSION ANALYSIS FOR A LOW COST ACTIVE DEBRIS REMOVAL DEMONSTRATION IN 2016

E. Joffre (1), **J. Forshaw** (2), **T. Secretin** (1), **S. Reynaud** (1), **T. Salmon** (3), **A. Pisseloup** (3), **G. Aglietti** (2)

(1) *Airbus Defence and Space, 66 Route de Verneuil, 78133 Les Mureaux, France*
@: eric.joffre@airbus.com - tel: +44-1438-77-3561
(2) *Surrey Space Centre, University of Surrey, Guildford, Surrey GU2 7XH, United Kingdom*
@: j.forshaw@surrey.ac.uk - tel: +44-1483-68-6307
(3) *Airbus Defence and Space, 3 rue du Général Niox, B.P. 20011, 33165 St Médard en Jalles Cedex, France*

Abstract: *Contracted by the European Commission in the frame of the EU's Seventh Framework Programme for Research (FP7), a wide European consortium has been working since 2013 towards the design of a low cost in-orbit demonstration called RemoveDEBRIS. With a targeted launch date in the second quarter of 2016, the RemoveDEBRIS mission aims at demonstrating key Active Debris Removal (ADR) technologies, including capture means (net and harpoon firing on a distant target), relative navigation techniques (vision-based navigation sensors and associated algorithms), and deorbiting technologies (drag sail deployment after the mission followed by an uncontrolled reentry). In order to achieve these objectives, a micro satellite test-bed will be launched into a Low Earth Orbit, where it will deploy its own dedicated targets and CubeSats to complete each demonstration. As part of its System Engineering role, Airbus Defence and Space has been conducting the Mission Analysis studies for this unprecedented mission. This paper will present a description of the RemoveDEBRIS demonstration objectives and scenario and will present in detail some specific mission related analyses and trade-offs that have driven the mission design.*

Keywords: *Mission Analysis and Design, Active Debris Removal, ADR, Capture Technologies, Navigation for Non-cooperative Rendezvous, Mission Opportunity Selection, Concept of Operations, CONOPS*

1. Introduction

RemoveDEBRIS is a low cost mission aiming to perform key Active Debris Removal (ADR) technology demonstrations including the use of a net, a harpoon, vision-based navigation and a dragsail in a realistic space operational environment, which is an important step towards a fully operational ADR mission [1, 2]. The project started in 2013 and is likely launching in 2016. For the purposes of the mission, CubeSats are ejected then used as targets instead of real space debris. This paper presents a detailed analysis of the mission trade-offs including orbit selection and astrodynamics, examination of lighting conditions and orbital lifetime.

1.1 Partners

The project consortium partners with their responsibilities are given in Tab. 1.

Table 1. RemoveDEBRIS Consortium Partners

Partner	Responsibility
SSC	Project management, CubeSats, Dragsail, Harpoon target assembly (HTA) structure
SSTL	Platform technical lead, Operations
Airbus DS France	System and Mission technical lead, Vision-Based Navigation (VBN)
Airbus DS Germany	Net
Airbus DS UK	Harpoon (HTA payload)
ISIS	CubeSat deployers
CSEM	LiDAR camera
Inria	VBN algorithms
Stellenbosch University	CubeSat avionics

1.2 Literature

In the field of ADR, there is a wide range of conceptual studies. ESA has produced a range of CleanSpace roadmaps, two of which focus on (a) space debris mitigation and (b) technologies for space debris remediation. ESA's Service Oriented ADR (SOADR) design phases involved the analysis of a mission that could remove very heavy debris from orbit examining both the technical challenges and the business aspects of multiple ADR missions [11, 12, 13]. ESA has conducted industrial phase-A an B studies, as well as internal exercises as part of the `e.Deorbit' programme, an element of the agency CleanSpace initiative [5]. ESA's Satellite Servicing Building Blocks (SBB) study originally examined remote maintenance of geostationary telecommunications satellites using a robotic arm [4]. Aviospace has also been involved with some ADR studies: the Capture and De-orbiting Technologies (CADET) study examined attitude estimation and non-cooperative approach using a visual and infra-red system. Airbus's and Aviospace's Heavy Active Debris Removal (HADR) study examined trade-offs for different ADR technologies, especially including flexible link capture systems. In addition to the various conceptual studies, a range of missions are planning to test specific ADR technologies.. Another mission is DLR's (German space agency) DEOS (Deutsche Orbital Servicing Mission) that aims to rendezvous with a non-cooperative and tumbling spacecraft by means of a robotic manipulator system accommodated on a servicing satellite [9]. CleanSpace One, a collaboration between EPFL and Swiss Space Systems (S3), aims to use microsatellites with a robotic arm to demonstrate ADR technologies [10]. Other missions of interest include the First European System for Active Debris Removal with Nets (ADR1EN), which aims to validate and qualify a net for space, and BETS (propellantless deorbiting of space debris by bare electrodynamic tethers) [16]. Among research programmes from major space agencies, there is also a range of smaller subsets of ADR literature. Chamot at MIT and EPFL have considered the design of three distinct architectures for debris removal depending on the level of chaser vehicle reusability [3]. The ion-beam shepherd is a potential debris removal solution that has been discussed extensively [8]. In addition, a focus on tether dynamics between chaser and target is becoming a wider area of interest [12, 7, 6]. Airbus DS has spent significant resources in the design of both net [19] and harpoon demonstrators for use in space. The net is considered by some studies to be the most robust method for debris removal, requiring the least knowledge about the target object [12]. Airbus DS is also involved in the development of vision-based relative navigation systems, which would be necessary for future debris removal missions [17].

1.3 Paper Structure

Section 2 provides an overview of the RemoveDEBRIS mission, platform and payloads. The paper then explores the orbital trade-offs including drag effects in Section 3 and lighting conditions in Section 4. The experimental mission analyses are then examined in Sections 5 and 6 which cover the VBN demonstration and net, harpoon demonstrations respectively. Finally the paper is concluded in Section 7.

2. Mission Baseline and Platform Overview

2.1 Launch

Two options have been considered for the launch:

- The first is to be launched as a piggyback payload in a Sun-Synchronous Orbit (SSO),
- The second option is to be launched in a Low Earth Orbit (LEO) from the International Space Station (ISS) by NanoRacks.

An extensive trade-off has been carried out regarding the launch strategy. Selection criteria include cost and availability of the launch provider, as well as accommodation constraints. Some of the mission related trade-offs will be further detailed in the next sections.

Even though the latter option was not considered initially, it may finally be the only option to fit into the budget allocated for the launch, solving in the meantime potential issues with the orbit lifetime (see Section 3), as well as the lighting conditions for the demonstrations (see Section 4). It is therefore considered as the current baseline launch option, raising platform design challenges including important mass and volume reduction with respect to the initial design.

2.2 In-Orbit Demonstrations

This section details the several in-orbit demonstrations of the mission. The three primary experiments are performed sequentially, with data from each being downloaded before the start of the next experiment. Mission operations are expected to last 40 weeks. The dragsail demonstration is undertaken last when the platform is to be de-orbited.

The net scenario is shown in Fig. 1 and is designed to help mature net capture technology in space. In this experiment, initially the first CubeSat (net), DS-1, is ejected by the platform at a low velocity (0.05 m/s). DS-1 proceeds to inflate a balloon which, as well as acting as a deorbiting technology, provides a larger target area. A net is then ejected at the balloon from the platform 140 s after the CubeSat ejection. Once the net hits the target, deployment masses at the end of the net wrap around and entangle the target and motor driven winches reel in the neck of the net preventing the re-opening of the net. The CubeSat is then left to deorbit at an accelerated rate due to the large surface area of the balloon.

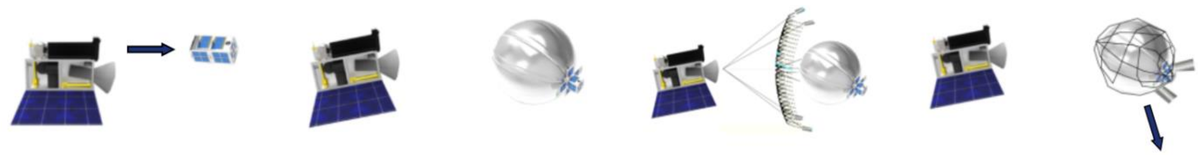

Figure 1. Net Demonstration Scenario

The harpoon is part of the HTA (Harpoon Target Assembly) experiment shown in Fig. 2. The payload uses a deployable target that extends outwards from the platform which is used as a target for the harpoon. The harpoon is designed with a flip-out locking mechanism that prevents the tether from pulling out of the CubeSat.

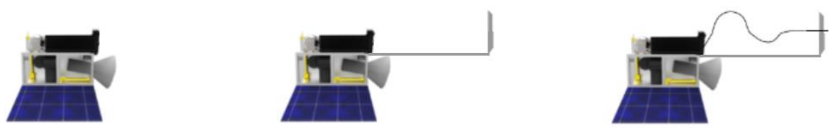

Figure 2. Harpoon Demonstration Scenario

The VBN experiment is shown in Fig. 3. In this experiment, the second CubeSat (VBN), DS-2, is ejected by the platform. The VBN system (including LiDAR) uses the previous net and harpoon experiments to calibrate itself. Attitude manoeuvres are then undertaken allowing the VBN system and supervision cameras to collect data and imagery which are later post-processed on ground.

Figure 3. VBN Demonstration Scenario

The dragsail is the fourth and final experiment. The 10 m² dragsail is used to de-orbit the platform at the mission end-of-life.

2.3 RemoveSAT Platform

The platform utilises the next generation of low earth orbit spacecraft avionics systems and structural design being developed at SSTL called the X50 series. The X50 architecture is based on a modular and expandable philosophy that utilises common modules. This allows the system to be adaptable to varying mission applications and requirements.

The platform, shown in Figure 4 and Figure 5, is based on four side panels, a payload panel, and a separation panel. Payloads are mounted either on the payload panel within the payload volume atop the avionics bay or along the side panels as required. The side and payload panels are made from aluminium honeycomb sandwich panels while the separation panel is made out of machined aluminium. Three of the four side panels are also populated with solar cells to provide power throughout the orbit. Below the payload panel is the platform avionics bay where the platform sub-systems are housed. This includes items such as magnetometers, magnetorquers, reaction wheels, gyros, on-board computers, GPS receiver, X50 avionics stack, and batteries.

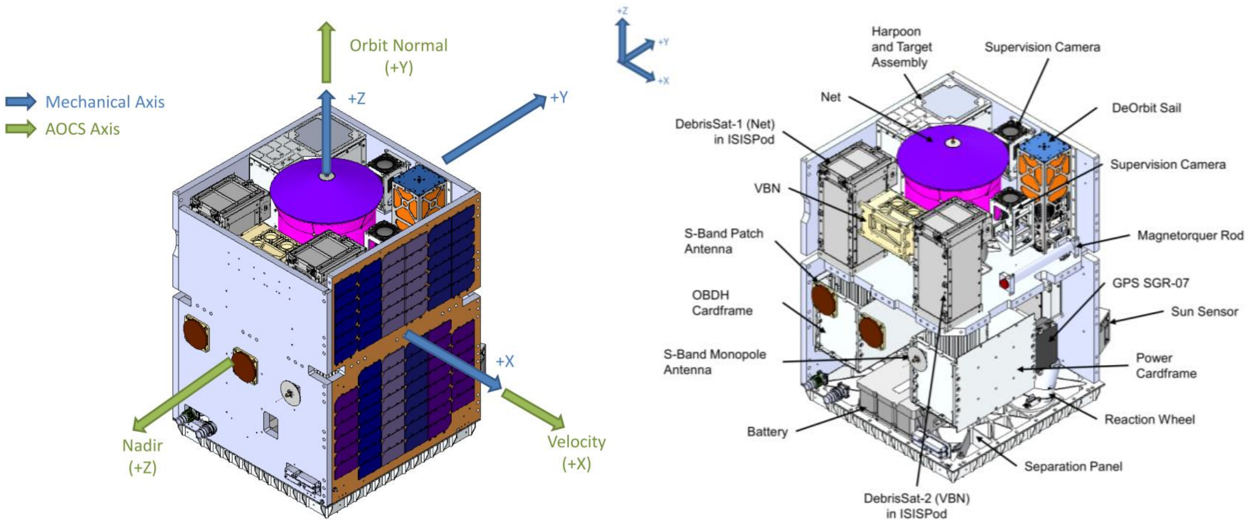

Figure 4. RemoveSAT Platform Layout and Main Subsystems

The X50 avionics system builds on the modular and expandable philosophy and also improves manufacturability, integration, and testing. The avionics system is based on a cardframe structure with backplane interconnections. This results in far less labour to interconnect the modules and also simplifies integration and module insertion and replacement. The new modules that have been developed for X50 avionics include: Power Distribution Module (PDM), Battery Charge Module (BCM), S-band Transmitter/Receiver (STRx), Payload Interface Unit (PIU), CAN Bridge.

3. Drag Effects on the Launch Opportunity Selection

In a various range of space applications, the most significant orbital perturbations with respect to the Keplerian dynamics model are those due to the non-sphericity of the Earth's gravitational potential, and especially to its first zonal coefficient J_2. In our case however, we will pay specific attention to the drag effects since, contrarily to the gravitation perturbations, they do not affect the platform and the different CubeSats in the same way. Indeed the *relative* perturbations must be considered when dealing with formation flying or rendezvous applications, and in Low Earth Orbit the relative drag effects can be critical when the different orbited spacecrafts have dissymmetric features. It has been numerically verified with Airbus DS in-house Mission Analysis simulation platform OSCAR [14] that, given the demonstration scenario and the orbited objects properties, the impact of the Earth's oblateness on the relative motion is insignificant as compared to the drag contribution.

In that sense, lower drag conditions seem to be advantageous for the RemoveDEBRIS demonstrations, all the more so as the poor knowledge of the atmospheric density (see Section 3.1) and the uncertainties in the orbited spacecrafts' ballistic coefficients (see Section 3.2) lead to highly dispersed trajectories, as will be shown in Section 5. On the other hand, a higher drag level ensures a natural reentry in an acceptable time (see Section 3.3) and the trade-off on the orbit selection must therefore take into account these two antagonistic aspects.

3.1 Solar Activity and Atmospheric Density

When considering long-term drag effects in the exo-atmospheric region, it is necessary to take into account the fluctuations of the solar activity. At a given altitude, these variations can indeed account for a factor of up to 100 between the minimal and the maximal atmospheric density. Figure 5 illustrates the correlation between the atmospheric density and the solar activity, commonly quantified by the F10.7 index that measures the daily flux at a 10.7 cm wavelength (near the peak of the radio emission from the sun). An important solar activity will result in a dense atmosphere, which can become dramatically thinner when the activity weakens. NASA periodically updates predictions of the solar flux in the years to come, and the right figure shows the predicted evolution of the F10.7 index in the next 15 years.

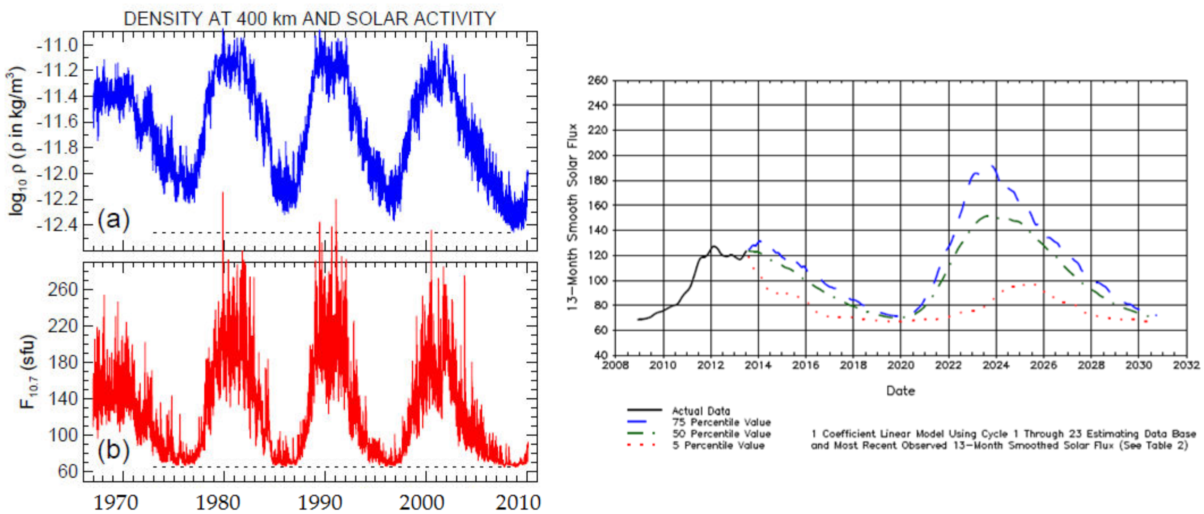

Figure 5. Solar Activity and Atmospheric Density Predictions (Credits: NASA)

In 2013, a peak of solar activity was reached, but as illustrated by the previous figure it actually proved to be historically low, probably the weakest over the past 100 years. With regard to these solar activity considerations, the foreseen date for the RemoveDEBRIS demonstration seems rather favourable: on one hand, the atmospheric density should be at a low level during the demonstrations (2016-2017 during which the F10.7 index should not exceed 110 sfu) thus minimising drag perturbations for the formation flying and capture operations, and on the other hand, it is expected to increase again a few years later, thus reducing the lifetime duration after the mission.

3.2 Relative Drag during the Demonstrations

The expression of the drag force experienced by an object is given by:

$$F = \tfrac{1}{2}\,\rho\, A\, C_D\, V^2 \qquad (1)$$

where ρ stands for the atmospheric density, V is the value of the object's velocity relative to the atmosphere, C_D is the drag coefficient and A the reference area (usually the cross-sectional area) for which the drag coefficient is given. By writing the expression of this force for both the RemoveSAT platform and for a target CubeSat, and after a division by the mass, the *relative drag acceleration* (of the RemoveSAT with respect to the CubeSat) can be expressed as:

$$a_D = \frac{1}{2} \rho V^2 \Delta B \tag{2}$$

ΔB differential ballistic coefficient $B_{\text{RemoveSAT}} - B_{\text{CubeSat}}$, B being defined for each vehicle as[1]:

$$B = A\, C_D / M \tag{3}$$

At a given altitude, both the atmospheric density and the relative velocity are imposed by the orbital parameters, and the only driving parameter is the differential ballistic coefficient.

Typically, a CubeSat will experience more drag than the platform, especially if it has panels (see section 5) that are oriented perpendicular to the relative velocity vector. Depending on its attitude, its cross-sectional area could indeed vary from a factor 1 to 10. Section 5 will provide a comprehensive analysis of the VBN demonstration with a Monte-Carlo analysis taking into account dispersions on the atmospheric density and ballistic coefficients. All simulations have been performed using the MSIS-86 Thermospheric Model [15] and assuming mean solar activity conditions in mid-2016.

3.3 Orbit Lifetime Estimation

As mentioned in the previous paragraph, the object that is likely to experience the weakest drag in orbit is the RemoveSAT itself. In case of a failure during the deployment of the sail designed to help with its deorbitation or in case of the absence of such a drag augmentation device, the platform should still reenter the Earth's atmosphere in less than 25 years after the end of the demonstration. Orbit lifetime simulations have been performed using the French Space Agency (CNES) tool STELA (*Semi-analytical Tool for End of Life Analysis*) that serves as a reference tool for the verification of the compliance with the French Space Act [18]. In the next table, the results of the simulations are shown for various initial altitudes and dates, in the case of a launch from ISS (51.6° inclination) or SSO.

Table 3. Orbit Lifetime

Orbit lifetime (years)		**End of mission date**			
		January 2017	**June 2017**	**January 2018**	**June 2018**
ISS - 51.6° Inclination	**330 km**	0.42	0.49	0.53	0.58
	370 km	1.20	1.40	1.52	1.66
	400 km	2.70	3.00	2.81	2.54
	435 km	4.30	4.10	3.63	3.29
SSO inclination	**500 km**	6.48	6.19	5.65	5.27
	550 km	14.76	14.67	14.00	13.71
	600 km	***27.32***	***26.72***	***26.39***	***25.72***

[1] The inverse convention is also used for the definition of the ballistic coefficient: $\beta = M/(AC_D)$, in which case it is expressed in kg/m².

It appears that the compliance with the 25 years rule is always achieved when launched from the ISS. If the RemoveSAT is jettisoned at a low altitude however, the orbit lifetime could be below one year, raising the concern of having too little time in orbit to download all the demonstrations data to the ground before re-entering into the atmosphere. On the other hand, the orbit lifetime and compliance to the Space Act is not granted in the SSO case as soon as the altitude is above 600 km in the absence of either a propulsive capability (deorbiting boost) or a drag augmentation device.

4. Lighting Conditions

The lighting conditions during the demonstrations are critical as they have a direct impact on the quality of the images acquired by a camera operating in the visible wavelengths. These images being used to assess the success of the demonstrations, it is of the utmost importance that the observed objects are properly lit by the sun. The lighting conditions will be described using the angles illustrated in Figure 6.

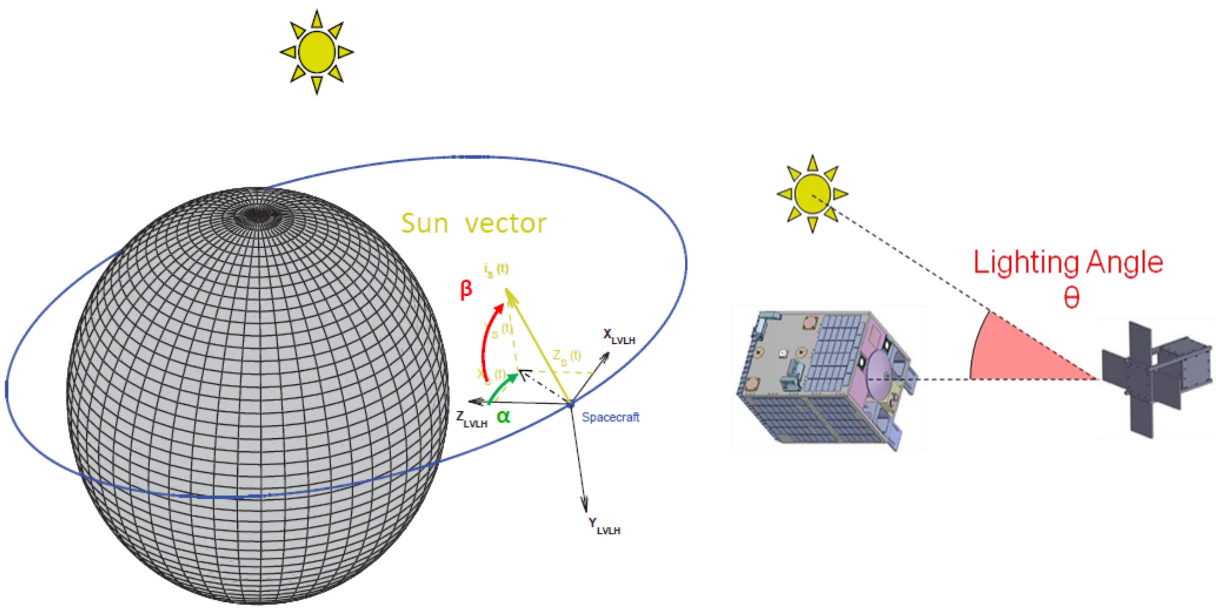

Figure 6. Solar Angles (α, β) and Lighting Angle (θ) Definitions

4.1 Description of the Lighting Conditions

Given that the relative motion dynamics analyses are performed in the platform's LVLH local coordinate system (Local Vertical Local Horizontal, illustrated on the left on Figure 6), it is relevant to study the local sunlight direction by means of the sun vector components in such a frame. To that end, two angles (α, β) are defined to study the time evolution of the sun vector as seen from the in-orbit spacecraft:

- The in-plane α angle represents the angle between the nadir and the projection of the sun vector in the orbital plane.
- The out-of-plane β angle is the angle between the orbital plane and the sun vector.

This choice of parameters is not arbitrary. Indeed, the solar β angle evolution is not only essential for the lighting conditions but also for the power analyses, as it is directly linked to the eclipses duration on a circular orbit. For a given β, the periods of eclipse correspond to certain values of the in-plane α angle when the Sun is below the horizon. Figure 7 below represents the duration of eclipses per orbit (Y axis), for various altitudes of a circular orbit, and as a function of the β angle (X axis).

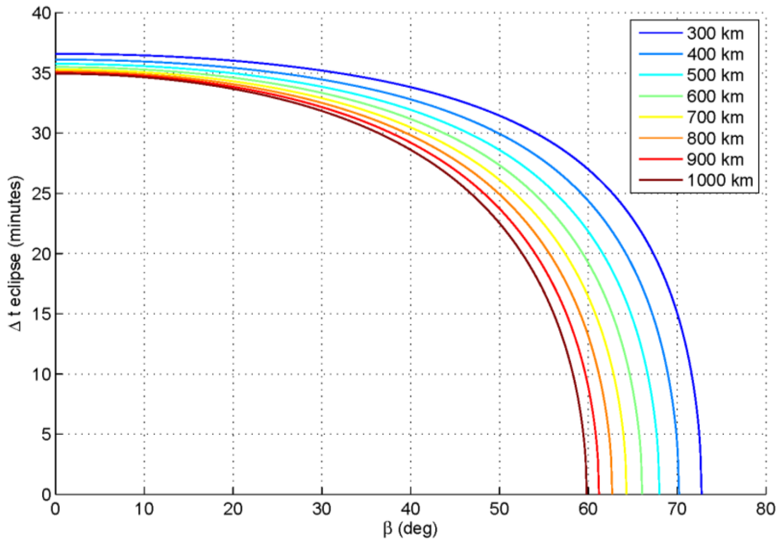

Figure 7. Eclipse Duration per Orbital Period on Circular Orbits

Another reason for this choice of parameters is that these two angles have very different variation rates. On one hand, the in-plane angle α has a short-term variation rate of one orbital period and it typically completes a full 360° revolution within 90 to 95 minutes in the considered range of altitudes. On the other hand, the out-of-plane angle β does not depend on the true anomaly, and it varies at a much lower rate. Indeed, on a circular orbit with a given inclination, β is essentially a function of the Right Ascension of the Sun, that completes a full revolution within one year, and of the Right Ascension of the Ascending Node, that typically drifts of a few degrees per day in LEO. Both these angles are illustrated in Figure 8.

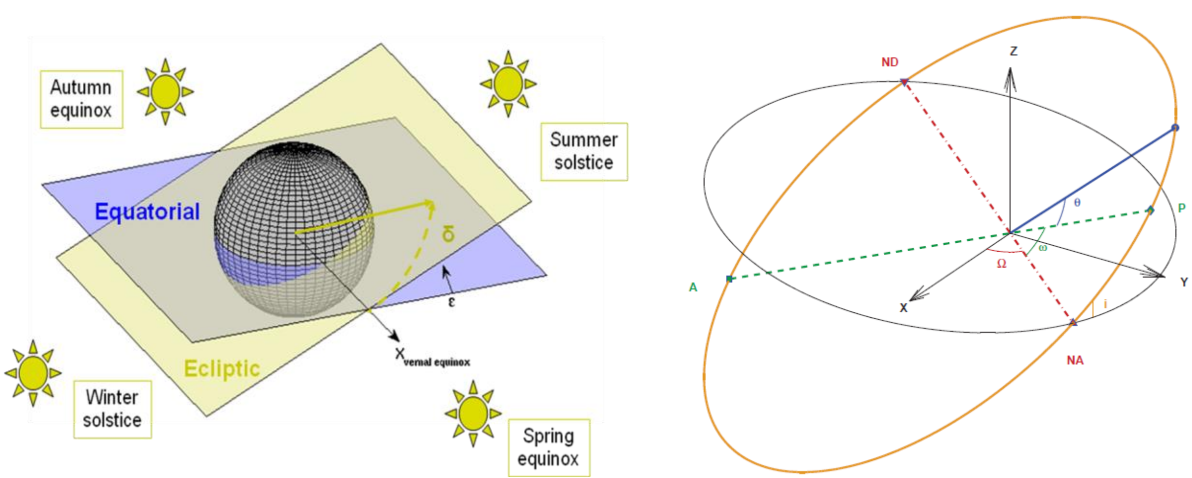

Figure 8. Right Ascension of the Mean Sun (δ), Right Ascension of the Ascending Node (Ω)

Instead of the Right Ascension of the Ascending Node, the *Mean Local Time of the Ascending Node (MLTAN)* will be used to describe the variation of the solar β angle. The MLTAN is expressed in hours, and can be defined as follows (assuming $\Omega - \delta$ is set between $-\pi$ and $+\pi$):

$$\mathrm{MLTAN} = 12 + (\Omega - \delta) \times 24/2\pi \qquad (4)$$

The Right Ascension of the Ascending Node of an orbit with inclination i, semi major axis a, mean motion n, and eccentricity e has a secular variation given by the next expression:

$$\frac{d\Omega}{dt} = -\frac{3}{2} J_2 n \left(\frac{R_T}{a}\right)^2 \frac{1}{\left(1-e^2\right)^2} \cos(i) \qquad (5)$$

where R_T is the Earth radius at the equator, and J_2 is the first zonal coefficient of the gravity force potential.

Lighting conditions are investigated by means of *maps* showing:

- The MLTAN between 0 h and 24 h, on the X-axis.
- The mean sun angle (or day angle) between 0° (spring equinox) and 360°, on the Y-axis.
- The β angle variation on this (MLTAN, δ) domain, as coloured isolines with the colour scale given on the right of the figure.
- An example trajectory in dim gray line. The initial conditions (MLTAN, δ) at launch being unknown, an arbitrary 12h MLTAN at spring equinox is assumed for the example below.

The first lighting map is provided for an ISS-like orbit at 400 km in Figure 9.

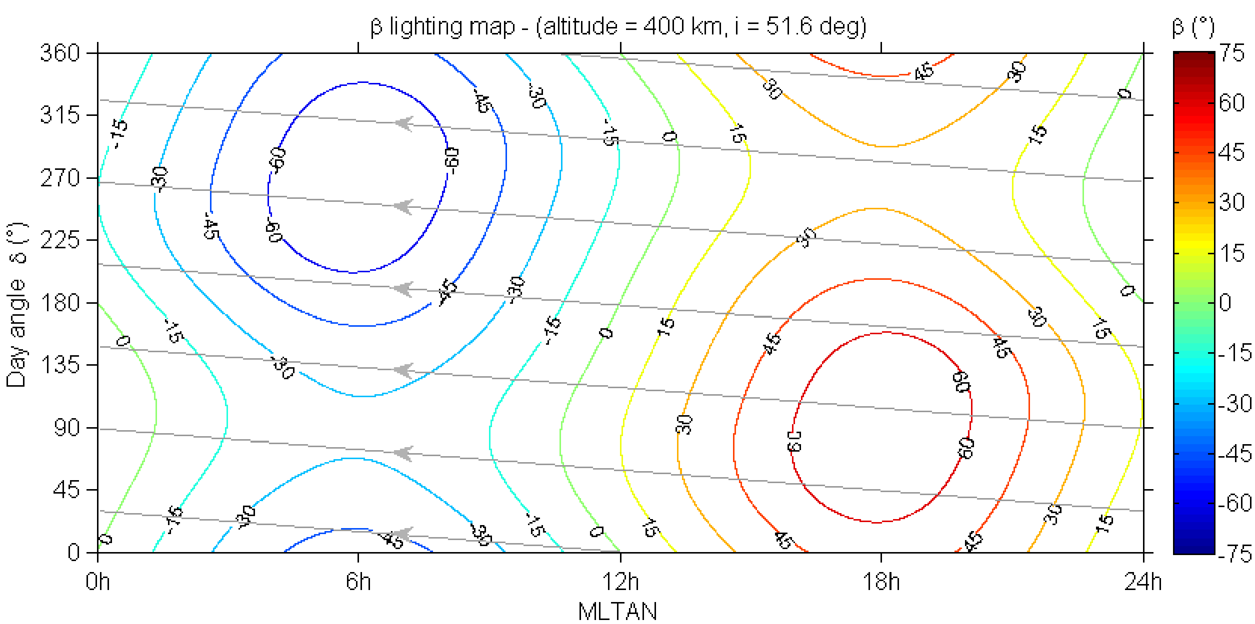

Figure 9. ISS-like Orbit β Lighting Map and Example Trajectory

By following the trajectory (gray line), one can read the β angle time evolution as actually seen by the spacecraft on its orbit. Figure 10 illustrates the variation of this angle over a year with the same initial conditions: on an ISS-like orbit, the solar β angle has a short-term period of about 2 months, and it varies between -75° (which would be reached if the orbit passed at a 6h MLTAN at the winter solstice) and +75° (18h MLTAN at the summer solstice).

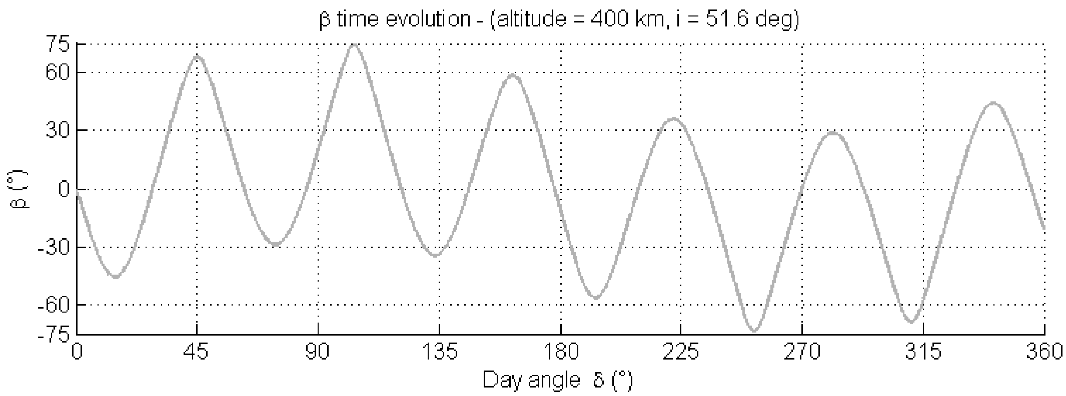

Figure 10. ISS-like Orbit - β Example Yearly Evolution

The case of Sun-Synchronous Orbits is very specific as by definition, such orbits are designed to have a constant MLTAN. Altitude and inclination are tuned together so that the secular drift rate of the Right Ascension of the Ascending Node equals the day angle variation rate (360° per year). On the β lighting map in Figure 11, provided for a 600 km SSO, it means that an example trajectory is represented by a vertical line.

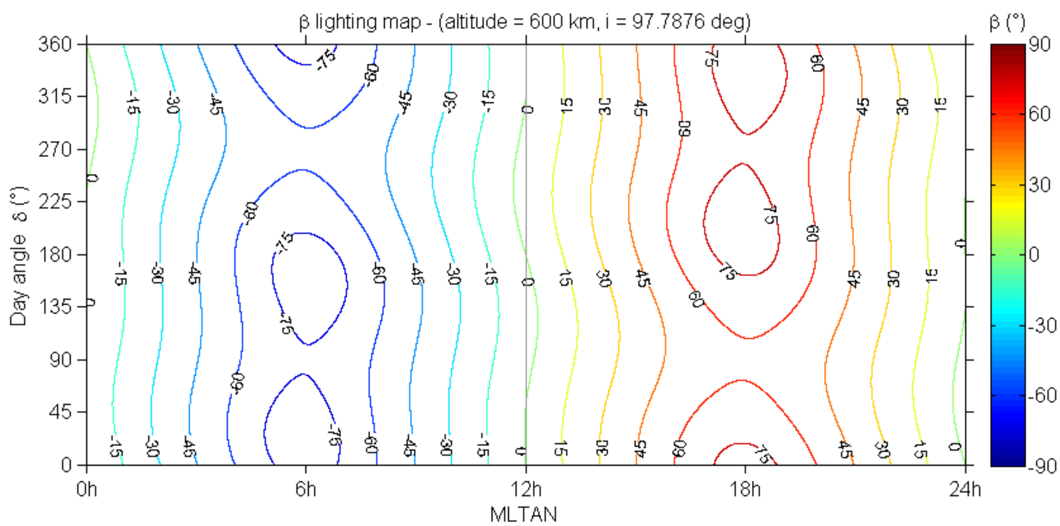

Figure 11. SSO Orbit β Lighting Map and Example Trajectory (Noon-Midnight Orbit)

In the case of SSO orbits, β can take all values between -90° and +90°. For a given MLTAN however, value that is set by the injection conditions and that remains constant afterwards, the solar β angle generally exhibits small variations. Figure 12 represents the time evolution on a 600 km with the same initial conditions (12h MLTAN or *noon-midnight* orbit).

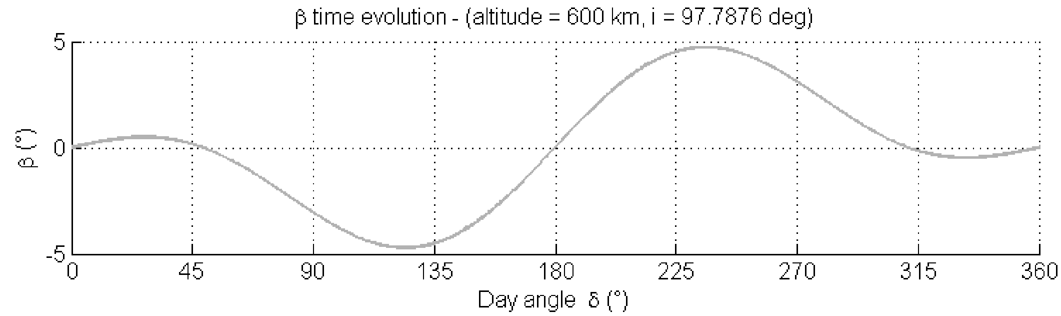

Figure 12. 600 km (Noon-Midnight) SSO - β Yearly Evolution

Another example,in Figure 13, is provided for a SSO with a MLTAN of 6 h (dawn-dusk), leading to the largest possible variations of β for this kind of orbits.

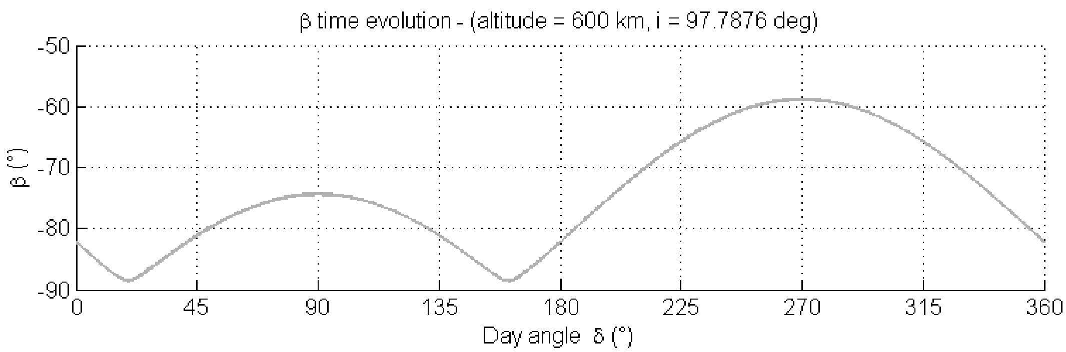

Figure 13. 600 km (Dawn-Dusk) SSO - β Yearly Evolution

4.2 Application to the RemoveDEBRIS Demonstration Opportunities

The results of the previous paragraphs have serious implications in the design of the RemoveDEBRIS mission. Indeed, optimal lighting conditions are reached if the lighting angle θ (see Figure 6) is kept below 45°. This angle depends on the (α, β) angles defining the local direction of the Sun on one hand, and on the local direction of the target as seen from the platform's camera on the other hand. As will be illustrated in the case of the VBN demonstration (Section 5), the target jettisoning direction (and then the resulting line of sight) is constrained by other factors and cannot be chosen freely, thus constraining the range of acceptable (α, β) pairs.

Regarding the launch option trade-off, this favours the ISS case since it offers the advantage of leading to greatly varying lighting conditions throughout the year, therefore leaving possible *opportunities* for the demonstrations:

- The acceptable out-of-plane β angle is reached by waiting the right period of time during the year (two months short-term period).
- The acceptable in-plane α angle is then reached by waiting the precise time on the orbit (true anomaly) for the demonstration to be triggered.

In the case of a SSO launch however, the lighting conditions are imposed by the launch provider, and they are therefore not chosen in the case of a piggyback launch. The resulting evolution of the lighting conditions could be incompatible with the demonstrations.

5. Vision Based Navigation Demonstration

In this section, a more detailed description of the Vision Based Navigation (VBN) demonstration scenario and the associated mission analyses are provided, assuming a launch from the ISS.

5.1 Demonstration Objectives and Baseline Scenario

The VBN demonstration aims at increasing the TRL of new generation relative navigation sensors considered as mission enablers for non-cooperative rendezvous [17]. Specifically, the RemoveDEBRIS platform will carry a Miniaturised LiDAR (MLiDAR) and a 2D optical camera that will be tested in an environment representative of an actual ADR mission. Relative navigation algorithms and image processing for the reconstruction of the relative attitude motion will be performed on ground after the mission. In order to provide a *truth* for the navigation and to assess the relative navigation algorithms performance, differential GPS measurements are recorded and sent by telemetry with the demonstration data. The CubeSat that is released and used as a target for the VBN demonstration (DS-2) is equipped with small panels, deployed just after the jettisoning so that its shape is more representative of a real satellite.

The initially foreseen demonstration scenario involved the ability to perform maneuvers around the target, and to keep a target-pointing attitude. This required active closed-loop attitude control relying on the measurements of a dedicated infra-red camera, and reaction wheels as actuators. In order to save some mass and to reduce the cost of the overall mission, the propulsive capability of the platform and closed-loop attitude control have been discarded. Consequently, the VBN demonstration simply consists in the release of a CubesSat in a predefined direction, followed by an open-loop attitude maneuvering of the platform. This ejection direction is optimised to maximise the success rate of the demonstration, defined as the probability to keep the target in the field of view of the camera, while meeting the constraints on the scenario. The following requirements have a direct impact on the demonstration scenario optimisation:

- The lighting angle shall remain less than 45° (3 σ) following separation and until the apparent size of the target is less than 50 pixels (distance of about 50 m).
- The target shall remain entirely in the field-of-view of the camera (16°) following separation until the apparent size of the target is less than 50 pixels.
- VBN acquisition with Earth background and with the target in the field-of-view shall be performed.
- A critical additional constraint is that the RemoveSAT and the CubeSat should not collide, in order to avoid the generation of additional debris.

Using the same angles as the ones described in Section 4 to describe the sun vector orientation, the optimisation of the target jettisoning has led to the following angles:

$$\alpha_{DS} = -115.5° \qquad (6)$$
$$\beta_{DS} = +/-67.7°$$

The sign of the β_{DS} angle does not matter as opposite values lead to symmetrical trajectories with respect to the local vertical plane. A positive angle corresponds to a jettisoning towards the left as seen from the platform (negative Y_{LVLH} component).

5.2 Opportunity Periods with respect to the Lighting Conditions

The ejection direction being selected, it is then possible to determine the set of solar local angles (α, β) that lead to acceptable lighting conditions at jettisoning:

- A minimum lighting angle of 20°: in case of a lighting angle below this value (near alignment of the sun, the platform and the target), the target would actually be in the shadow of the platform at the beginning of the demonstration.
- A maximum lighting angle of 45° as stated in the requirements.

With the selected ejection direction (Equation 6), the acceptable solar angle (α, β) can be represented on a two-dimensional domain. Figure 14 shows the map for the lighting angle θ (coloured isolines) in the α (X-axis), β (Y-axis) domain. The gray regions correspond to eclipse conditions at 400 km. The admissible region in blue corresponds to the set of (α, β) pairs leading to a lighting angle comprised between 20° and 45°, and not in eclipse. Only the negative part of the solar β values are represented, corresponding to a DS jettisoning towards the left (-Y) as seen from the platform's orbital velocity. The other part (β > 0°) would be symmetrical considering an opposite ejection direction for the target, that is to say β_{DS} = -67.7°, towards the right (+Y).

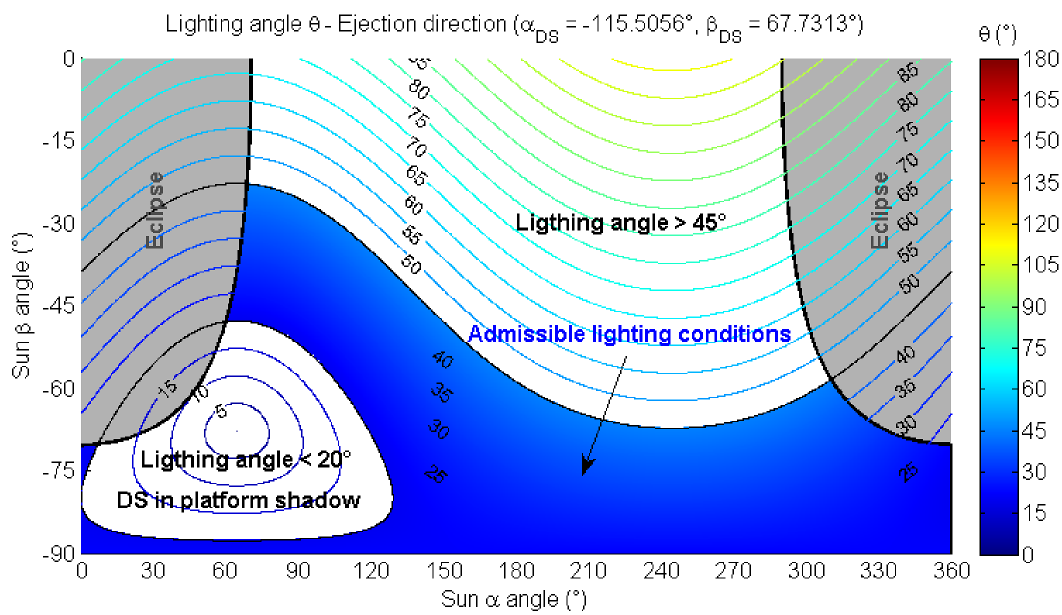

Figure 14. Admissible Solar Angles (α, β) for the VBN Demonstration

However, this is only applicable for the first instants of the demonstration. Because of the orbital dynamics governing the relative motion of the target with respect to the platform (including the relative drag), the line of sight of the DebrisSAT will quickly deviate from its initial direction. The local solar angles will evolve too. The optimisation of the ejection direction must consider the remaining of the demonstration, trying to keep good lighting conditions as long as possible. Results will be presented in the next paragraph (see Figure 18). Eventually, it has been determined that optimal lighting conditions for the VBN demonstration are obtained for:

$$|\beta_{SUN}| = 40° \text{ +/- } 5° \quad (7)$$

Figure 15 represents the corresponding opportunity regions on the lighting map described in Section 4, for the two admissible values of β_{DS}. The dashed line represents again an example trajectory over one year, from the bottom to the top of the figure.

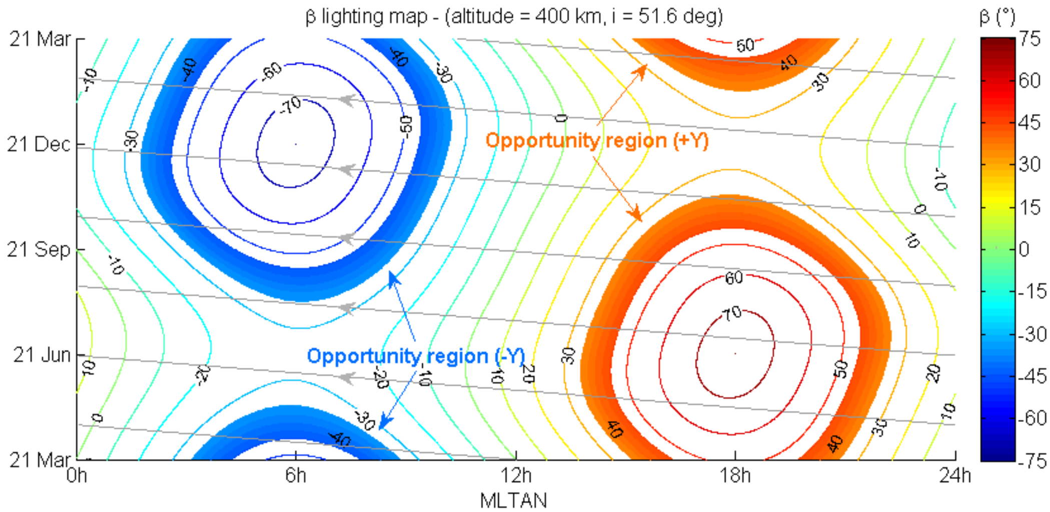

Figure 15. VBN Demonstration Opportunity Map

In any of the two opportunity regions, the demonstration must be triggered at a specific position on the orbit (true anomaly) so that the solar in-plane angle α is within the admissible range (see Figure 14). The optimal value for the solar in-plane angle α is:

$$\alpha_{SUN} = 64.5° \qquad (8)$$

The previous opportunity map shows that there are at least two opportunities periods for the VBN demonstration every two months, lasting typically two days. Periods without opportunity do not last much than 1 month around the solstices and there are two periods of opportunities per month around the equinoxes.

5.3 Monte Carlo Simulations

Monte-Carlo simulations have been performed to simulate the relative motion trajectories and the evolution of the lighting conditions, while considering several dispersions on the VBN demonstration scenario. The following assumptions were considered:

- Altitude = 400 km
- Atmospheric density: gaussian distribution around the nominal value from MSIS-86 Thermospheric Model: $1\sigma = 100\%$
- Ballistic coefficient dispersion for each satellite: $1\sigma = 10\%$ (gaussian)
- CubeSat deployer ejection ΔV, magnitude : $3\sigma = 10\%$ (gaussian)
- CubeSat deployer ejection ΔV, direction accuracy : $3\sigma = 5°$ (gaussian)
- Platform absolute pointing accuracy before jettisoning: $3\sigma = 5°$ (gaussian)

The following figures represent the resulting dispersed LVLH trajectories of the DebrisSAT DS-2 with respect to the platform (red curves). The blue curve represents the nominal trajectory, and the green one the drag-free trajectory. Black portions correspond to parts of the orbit when the Earth is in the line of sight (platform to target).

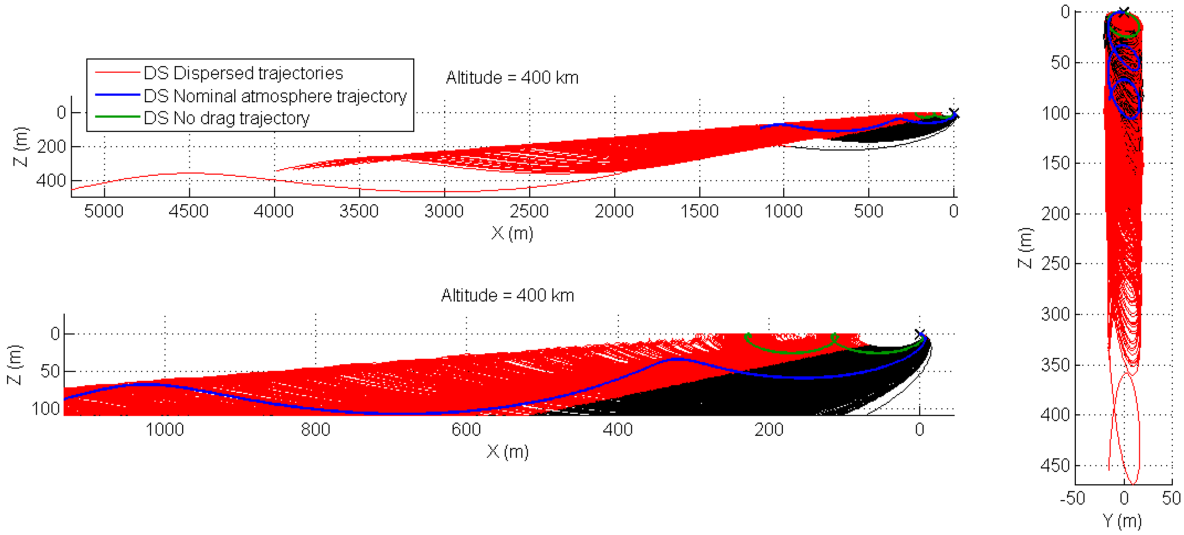

Figure 16. Dispersed Trajectories – In-plane XZ (top-left, zoom: bottom left) Out-of-plane YZ (right)

The next figure shows the corresponding evolution of the distance for the beginning of the demonstration. It shows that, despite the high level of dispersions, no trajectory comes back close enough to actually risk a collision with the platform.

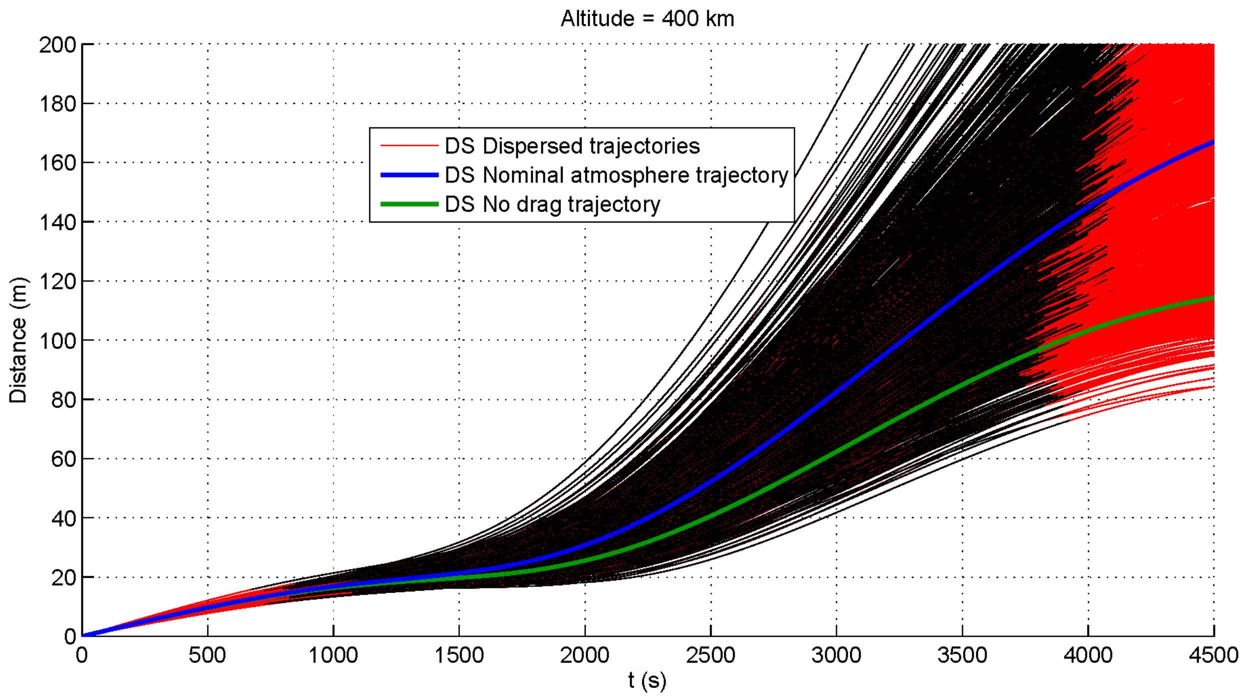

Figure 17. Dispersed Trajectories - Distance

The next figure illustrates the evolution of the lighting angle, assuming nominal conditions at jettisoning (see Equations 6 to 8).

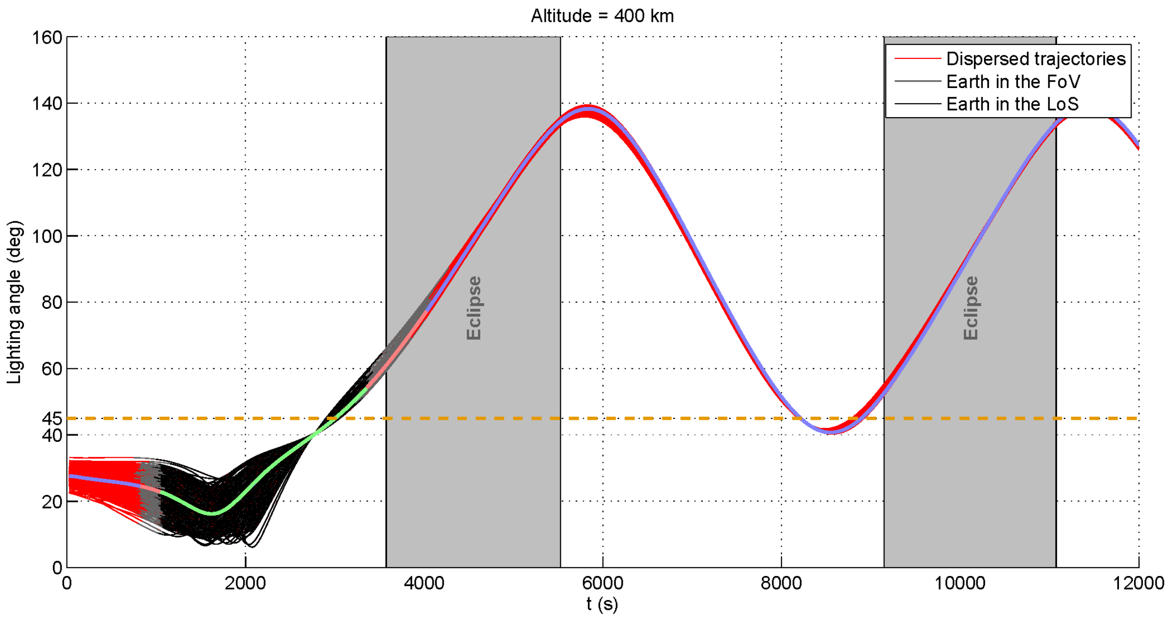

Figure 18. Lighting Conditions: Lighting Angle and Eclipse Periods

From Figure 18, it can be seen that:

- Optimal lighting conditions are assured for all the dispersed trajectories during at least one hour (3600 s) after the target jettisoning.
- Figure 17 shows that after this duration, all trajectories are further away than 50 m, ensuring that the first requirement in Section 5.1 is met.
- During this period (short-range demonstration), the target is initially seen with a black sky background.
- After approximately 10 minutes, the transition from black sky to Earth background occurs, while keeping optimal lighting conditions.
- Eclipses will not jeopardise the demonstration as they always occur when the lighting angle is not favourable anyway.
- It is theoretically possible to have good observation conditions of the target at far range after 8000 s when the lighting angle passes below 45° again.

Finally, the two last figures (19 and 20) illustrate the outcome of the pointing strategy. As described above, the attitude profile of the platform will be performed in open-loop as there is no dedicated sensor to perform an active closed-loop attitude control. The strategy consists in following the nominal attitude profile *from the initial dispersed attitude*[2] by means of gyrometric measurements and reaction wheels control. The next figure shows the resulting depointing, that must be kept below 8° (half field of view of the camera) as long as possible.

[2] The actual initial attitude of the platform is not the nominal attitude because of the errors from the absolute attitude sensors (Earth and Sun sensors, $3\sigma = 5°$).

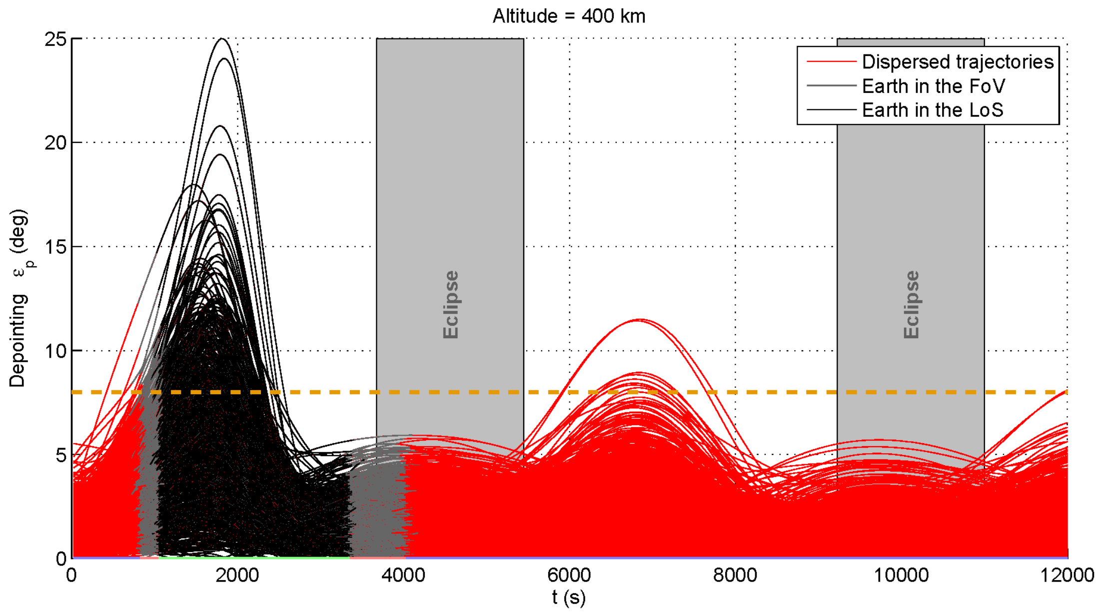

Figure 19. Dispersed Trajectories – Depointing

Figure 20 represents the percentage of trajectories actually within the field of view, or success rate, at each date of the early demonstration.

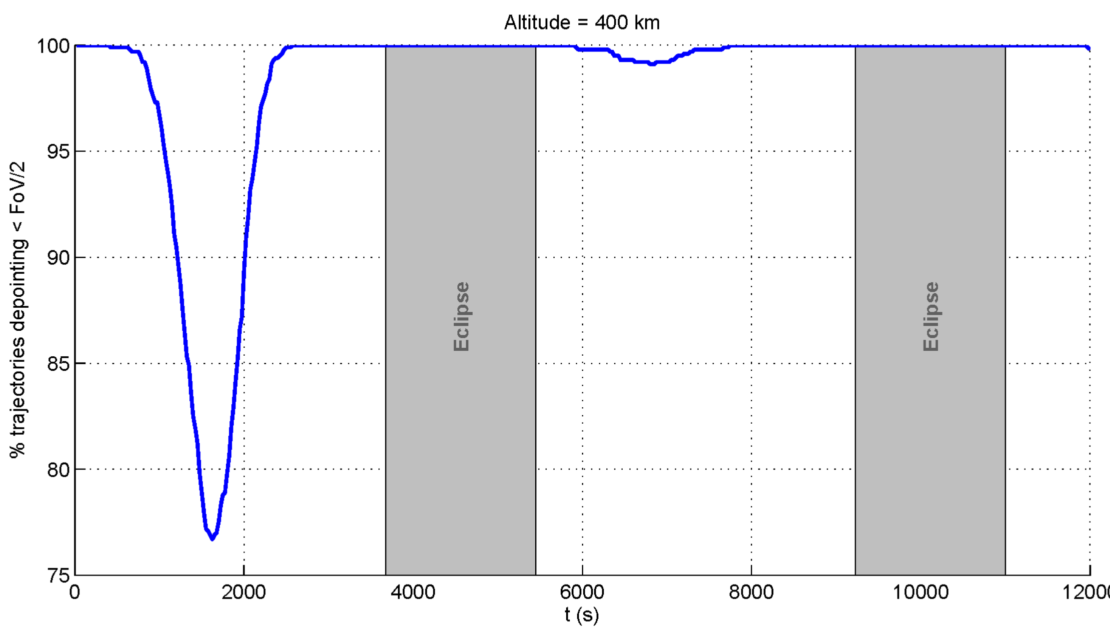

Figure 20. Dispersed Trajectories – Success Rate

The previous results show that the optimised baseline scenario for the VBN demonstration allows the initial objectives to be met despite the few degrees of freedom available and the importance of the dispersions on the trajectories.

6. Net and Harpoon Demonstrations

The study of the opportunities for the net demonstration is more straightforward than for the VBN demonstration since good lighting conditions are only required for a very short period of time after the target jettisoning (see Section 2.2). It is also the case for the harpoon demonstration. The main results are presented in this section, assuming here again that the mission is performed on an ISS-like orbit.

Like for the VBN demonstration, a critical constraint on the net scenario is that there is no risk of collision between the CubeSat and the platform, even when considering the worst-case dispersions on the ejection direction, due to the deployer inaccuracy and the initial attitude error of the platform. This condition is simply ensured in the short-term by setting a backward ejection component of the CubeSat in the local horizontal plane $(X,Y)_{LVLH}$ with a minimal angle of 10° with respect to the transverse axis. Since the platform experiences less drag than the target and the net, the relative drag will naturally increase the distance between the objects, therefore also ensuring long-term safety. The ejection directions envisaged for these demonstrations are illustrated in Figure 21 below.

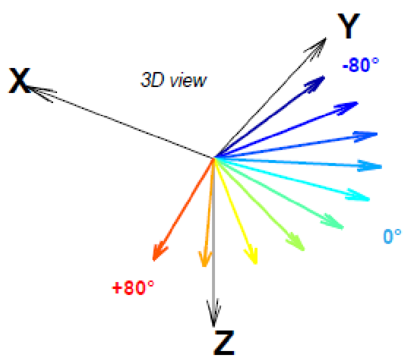

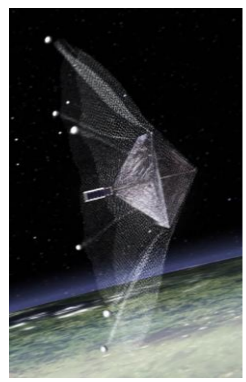

Figure 21. Possible Ejection Directions for the Net CubeSat (left) – Illustration of Net Capture (right)

This wide range of possibilities for the ejection direction leaves many opportunities to perform the demonstration with good lighting conditions. It is therefore possible to add a constraint to the scenario by imposing the net demonstration to be triggered when passing above the ground station in Guildford[3] in order to have real time images of the demonstration sequence. For a given day in the year (and therefore a given value for the solar β angle), this option sets the value of the solar in-plane α angle because the ground access occurs for a specific true anomaly on the orbit. If α is such that the platform is actually in eclipse, it is not possible to perform the demonstration. If not, it may be possible to find an ejection direction among the candidate directions that leads to good lighting conditions (lighting angle between 20° and 45°) to observe the scene with a supervision camera and ground visibility, in order to assess the success of the demonstration.

[3] On an ISS-like orbit there are typically four ground accesses per day from the Guildford ground station (latitude: 51.2431° longitude: -0.588°, minimal elevation for acquisition: 5°).

Figure 21 updates the opportunity map with the opportunity regions for the net/harpoon demonstrations. The black region corresponds to eclipse conditions when passing above the ground station in Guildford from a 400 km circular orbit inclined at 51.6°. The blue region shows the opportunity periods for the Net or Harpoon demonstrations, where there exists an admissible ejection direction leading to good lighting conditions at jettisoning.

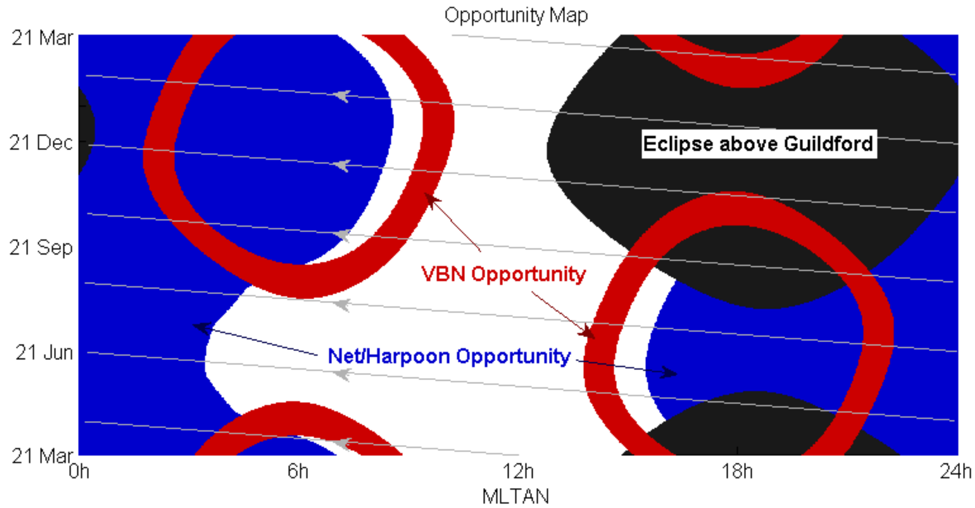

Figure 21. Opportunity Map for all Demonstrations

From this map, one can see that there are many opportunities throughout the year to perform the net/harpoon demonstration with live coverage from the ground. The longest periods of unavailability occur near the summer solstice and do not last more than one month.

7. Conclusion

In summary, RemoveDEBRIS is aimed at performing key ADR technology demonstrations (e.g. capture, deorbiting) representative of an operational scenario during a low-cost mission using novel key technologies for future missions in what promises to be the first ADR technology mission internationally. Key ADR technologies for debris removal include the use of harpoon and net to capture debris, vision-based navigation to target debris and a dragsail for deorbiting. Although this is not a fully-edged ADR mission as CubeSats are utilised as artificial debris targets, the project is an important step towards a fully operational ADR mission. The mission proposed is a vital prerequisite in achieving the ultimate goal of a cleaner Earth orbital environment. This paper has provided an overview of the mission and platform, with a key focus on the mission trade-offs. The analyses of the drag effects and the lighting conditions give advantage to a launch from the ISS, as compared to a launch as a piggyback payload in SSO for which unfavourable conditions at injection (imposed by the launcher) could be incompatible with the mission constraints. A baseline scenario has been established for all the demonstrations including the ejection directions of the CubeSats, and opportunity periods have been identified. The actual opportunities that will be eventually selected for each demonstration depend on the exact launch date of the mission, as well as the initial altitude and MLTAN. They will therefore be derived from the opportunity maps as soon as the launch conditions are confirmed.

The RemoveDEBRIS mission is currently in the 2nd year of the project. Design work is continuing and a range of EMs and QMs (Engineering and Qualification Models) have undergone testing. The platform providers aim to start receiving FMs (Flight Models) for payloads late 2015 and early 2016, with a launch currently targeted in late 2016.

The RemoveDEBRIS mission intends to fully comply with all relevant national and international space laws. In particular, it is of prime importance that all space elements released into orbit deorbit within 25 years. The very low altitude chosen means objects deorbit very quickly and adds extra safety to the mission than selection of a higher altitude. CubeSats are used here as artificial debris targets. This avoids any legal issues with targeting, capturing or deorbiting debris that is legally owned by other entities. The RemoveDEBRIS consortium aims to work with the EU, UK Space Agency (UKSA), ESA, CNES and other agencies/entities to provide the latest project achievements, incorporate their feedback, communicate and interface with them on all necessary regulatory procedures required for the RemoveDEBRIS mission.

8. Acknowledgements

This research is supported by the European Commission FP7-SPACE-2013-1 (project 607099) `RemoveDEBRIS - A Low Cost Active Debris Removal Demonstration Mission', a consortium partnership project consisting of: Surrey Space Centre (University of Surrey), SSTL, Airbus DS GmbH, Airbus SAS, Airbus Ltd, ISIS, CSEM, INRIA, Stellenbosch University.

9. References

[1] V. J. Lappas, J. L. Forshaw, L. Visagie, A. Pisseloup, T. Salmon, E. Joffre, T. Chabot, I. Retat, R. Axthelm, S. Barraclough, A. Ratcliffe, A. Bradford, H. Kadhem, N. Navarathinam, J. Rotteveel, C. Bernal, F. Chaumette, A. Pollini, W. H. Steyn, RemoveDEBRIS: An EU low cost demonstration mission to test ADR technologies, in: *65th International Astronautical Congress*, Toronto, Canada, 2014.

[2] J. L. Forshaw, G. Aglietti, N. Navarathinam, H. Kadhem, T. Salmon, E. Joffre, T. Chabot, I. Retat, R. Axthelm, S. Barraclough, A. Ratcliffe, C. Bernal, F. Chaumette, A. Pollini, W. H. Steyn, An in-orbit Active Debris Removal Mission - RemoveDEBRIS: Pre-Launch Update, in: *66th International Astronautical Congress*, Jerusalem, Israel, 2015.

[3] B. Chamot. Mission and system architecture design for active removal of rocket bodies in low earth orbit. Master's thesis, Massachusetts Institute of Technology, US, August 2012.

[4] C. Cougnet, B. Gerber, C. Heemskerk, K. Kapellos, and G. Visentin. On-orbit servicing system of a geo satellite fleet. In *9th ESA Workshop on Advanced Space Technologies for Robotics and Automation `ASTRA 2006'*, ESTEC, Netherlands, November 2006.

[5] European Space Agency. e.Deorbit CDF Study Report. Technical Report CDF-134(A), European Space Agency, 2012.

[6] Lee Z. Jasper and Hanspeter Schaub. Input shaped large thrust maneuver with a tethered debris object. In *6th European Conference on Space Debris*, number 6a.O-11, ESOC, Darmstadt, Germany, April 2013.

[7] Lee Z. Jasper, Carl R. Seubert, Hanspeter Schaub, Trushkyakov Valery, and Evgeny Yutkin. Tethered tug for large low earth orbit debris removal. In *American Institute of Aeronautics and Astronautics Astrodynamics Specialists Conference*, number AAS 12-252, San Diego, US, January 2012.

[8] M. Merino, E. Ahedo, C. Bombardelli, H. Urrutxua, J. Pelaez, and L. Summerer. Space debris removal with an ion beam shepherd satellite: target-plasma interaction. In *47th AIAA/ASME/SAE/ASEE Joint Propulsion Conference & Exhibit*, San Diego, US, August 2011.

[9] D. Reintsema, B. Sommer, T. Wolf, J. Theater, A. Radthke, W. Naumann, P. Rank, and J. Sommer. DEOS - The in-flight technology demonstration of german's robotics approach to dispose malfunctioned satellites. In ESA *11th Symposium on Advanced Space Technologies in Robotics and Automation*, ESTEC, Netherlands, April 2011.

[10] M. Richard, L. Kronig, F. Belloni, S. Rossi, V. Gass, C. Paccolat, J.P. Thiran, S. Araomi, I. Gavrilovich, and H. Shea. Uncooperative rendezvous and docking for microsats : The case for cleanspace one. In *6th International Conference on Recent Advances in Space Technologies (RAST)*, Istanbul, Turkey, June 2013.

[11] C Saunders, A. Chiesa, J. L. Forshaw, B. Parreira, and R. Biesbroek. Results of a system feasibility study on a heavy active debris removal mission. In CNES *3rd European Workshop on Space Debris Modeling and Remediation*, Paris, France, June 2014.

[12] C. Saunders, J. L. Forshaw, V. J. Lappas, A. Chiesa, B. Parreira, and R. Biesbroek. Mission and systems design for the debris removal of massive satellites. In *65th International Astronautical Congress*, Toronto, Canada, September 2014.

[13] C. Saunders, J. L. Forshaw, V. J. Lappas, D. Wade, D. Iron, and R. Biesbroek. Business and economic considerations for service oriented active debris removal missions. In *65th International Astronautical Congress*, Toronto, Canada, September 2014.

[14] B. Correia da Costa, M. Cerf, G. Dodelin, M. Fessard, and S. Reynaud. Extensive suite for efficient and accurate generic mission analyses. In *5th International Conference on Astrodynamics Tools and Techniques,* Noordwijk, The Netherlands, May 2012.

[15] Hedin, Alan E., Journal of Geophysical Research (ISSN 0148-0227), vol. 92, May 1, 1987, p. 4649-4662.

[16] Juan Ramon Sanmartin Losada, Mario Charro, Enrico C Lorenzini, Giacomo Colombatti, Jean-Francois Roussel, Pierre Serrath, John D Williams, Kan Xie, Francisco Garcia de Quiros, Jose A Carrasco, et al. Bets: Propellantless deorbiting of space debris by bare electrodynamic tethers. 2012.

[17] K. Kanani, A. Petit, E. Marchand, T. Chabot, B. Gerber. Vision-based navigation for debris removal missions. In *63rd International Astronautical Congress*, Naples, Italia, September 2012.

[18] Compliance of disposal orbits with the French Space Act: The Good Practices and the STELA Tool, C. Le Fèvre, H. Fraysse et al, IAC-12-A6.4.1

[19] Astrium Space Transportation. ROGER Phase-A Final Report Executive Summary. Technical Report ROG-SIBRE-EXS, Astrium Space Transportation, 2003.